

Printed March 1982

Thermal Fatigue Tests of 'Solar One' Receiver Tube Weldments

Darcy A. Hughes

Prepared by
Sandia National Laboratories
Albuquerque, New Mexico 87185 and Livermore, California 94550
for the United States Department of Energy
under Contract DE-AC04-76DP00789

Issued by Sandia Laboratories, operated for the United States Department of Energy by Sandia Corporation.

NOTICE

This report was prepared as an account of work sponsored by the United States Government. Neither the United States nor the United States Department of Energy, nor any of their employees, nor any of their contractors, subcontractors, or their employees, makes any warranty, express or implied, or assumes any legal liability or responsibility for the accuracy, completeness or usefulness of any information, apparatus, product or process disclosed, or represents that its use would not infringe privately owned rights.

Printed in the United States of America
Available from
National Technical Information Service
U. S. Department of Commerce
5285 Port Royal Road
Springfield, VA 22161
Price: Printed Copy \$4.50 ; Microfiche \$3.00

THERMAL FATIGUE TESTS OF "SOLAR ONE"
RECEIVER TUBE WELDMENTS

Darcy A. Hughes
Materials Science Division
Sandia National Laboratories, Livermore

ABSTRACT

Tubing for "Solar One" receiver panels is joined by longitudinal welds using a low heat input welding process. Concern existed that lack-of-fusion defects (crack-like notches at the root of the weld) created by this welding process would propagate during diurnal thermal cycling. If crack propagation occurred at these defects, it could shorten the life of the receiver tube panels. An experiment which simulated key elements of the receiver cyclic thermal strain environment was designed to address this concern. During the experiment, receiver tube weldments (welds prepared in the laboratory) were thermally cycled for 15,000 cycles. They were subsequently examined metallographically for crack propagation. Results of this examination revealed that no crack propagation occurred during the test.

CONTENTS

	<u>Page</u>
Introduction	9
Experimental Procedures	12
Results and Discussion	16
Summary and Conclusions	27
REFERENCES	28
APPENDIX	29

FIGURES

<u>Figure</u>		<u>Page</u>
1	Micrograph of lack-of-fusion weld defect prior to testing.	10
2	Average coefficient of thermal expansion for IN82 weld metal and alloy 800 versus temperature.	11
3	Thermal cycling apparatus for receiver tube weldments.	13
4	Close-up of radiant furnace and specimen.	14
5	Receiver tube weldment specimens for test.	15
6	Typical temperature history of weldment specimen for one cycle.	17
7	Variation of temperature along the length of specimens at peak temperature.	18
8	Lack-of-fusion weld defect, specimen removed after 5000 cycles.	19
9	Lack-of-fusion weld defect, specimen removed after 10,000 cycles.	20
10	Lack-of-fusion weld defect, specimen removed after 15,000 cycles.	21
11	Example of solidification crack in GTA tack weld, crack occurred during welding. Specimen tested for 10,000 cycles.	22
12	EDM flaws and lack-of-fusion weld defect, specimen removed after 10,000 cycles.	24
13	SEM micrograph of fractured surface showing lack-of-fusion region. Specimen notched and pulled apart after testing.	25
14	Schematic of strain/stress modes present at lack-of-fusion weld defects during test.	26

ACKNOWLEDGMENT

I would like to thank P. J. Royval and D. V. Zanini for the design and construction of the test apparatus, S. L. Robinson for his helpful ideas during the design of this test, J. C. Lippold and R. A. Bell for their consultation and welding assistance, and C. Imhoff for experimental assistance.

THERMAL FATIGUE TESTS OF "SOLAR ONE" RECEIVER TUBE WELDMENTS

Introduction

The central receiver for the 'Solar One' power plant is comprised of 24 tube panels of seventy tubes each which operate as once-through boilers by absorbing solar radiation. For optimum operation, the tube panels were designed to prevent radiant "shine-through" and to maximize thermal conduction between tubes. Thus, the tubing in the receiver panels was joined by longitudinal welds using a low heat input welding process.

There was concern that the lack-of-fusion defects (crack-like notches at the root of the weld, Fig. 1) created by this welding process could propagate during diurnal thermal cycling. The direction of such possible crack propagation was also of importance because through-wall cracking may be more detrimental than longitudinal unzipping of the welds. Both crack growth rate and propagation direction are determined by the cyclic thermal stress state at the tip of the defects induced by differential thermal expansion. The differential expansion results from the combined effect of one-sided heating and different coefficients of thermal expansion between the alloy 800 base metal and IN82 weld metal (Fig. 2). The complexity of the stress state and history precluded an analytical assessment of the extent of possible crack growth; thus, a laboratory experiment was designed and set up to address this problem.

One objective of this study was to construct the simplest experiment which would test a number of weld parameters in a reasonable time while still preserving the key elements of pilot plant operation as they pertain to weldment cracking. These key elements were determined to include single-sided heating, a temperature difference (ΔT) between the tube front and back at the peak temperature portion of the thermal cycle, and constraint against thermal expansion-induced bending.¹ A worst-case test condition of 621°C (1150°F) peak temperature at the tube crown and 510°C (950°F) on the back side of the tubing (at the weld) was chosen. This choice reflected both the 111°C (200°F) front-to-back ΔT calculated by MacDonell Douglas^{2,3} in the superheat region of the receiver panel and the maximum allowable design temperature of 621°C (1150°F). During the test, the tube assemblies were cycled between these peak temperatures and 65°C (150°F). Since the cyclic nature of these stresses was presumed to have the greatest effect on potential damage, the effects of hold periods at peak temperature and internal pressure were neglected.

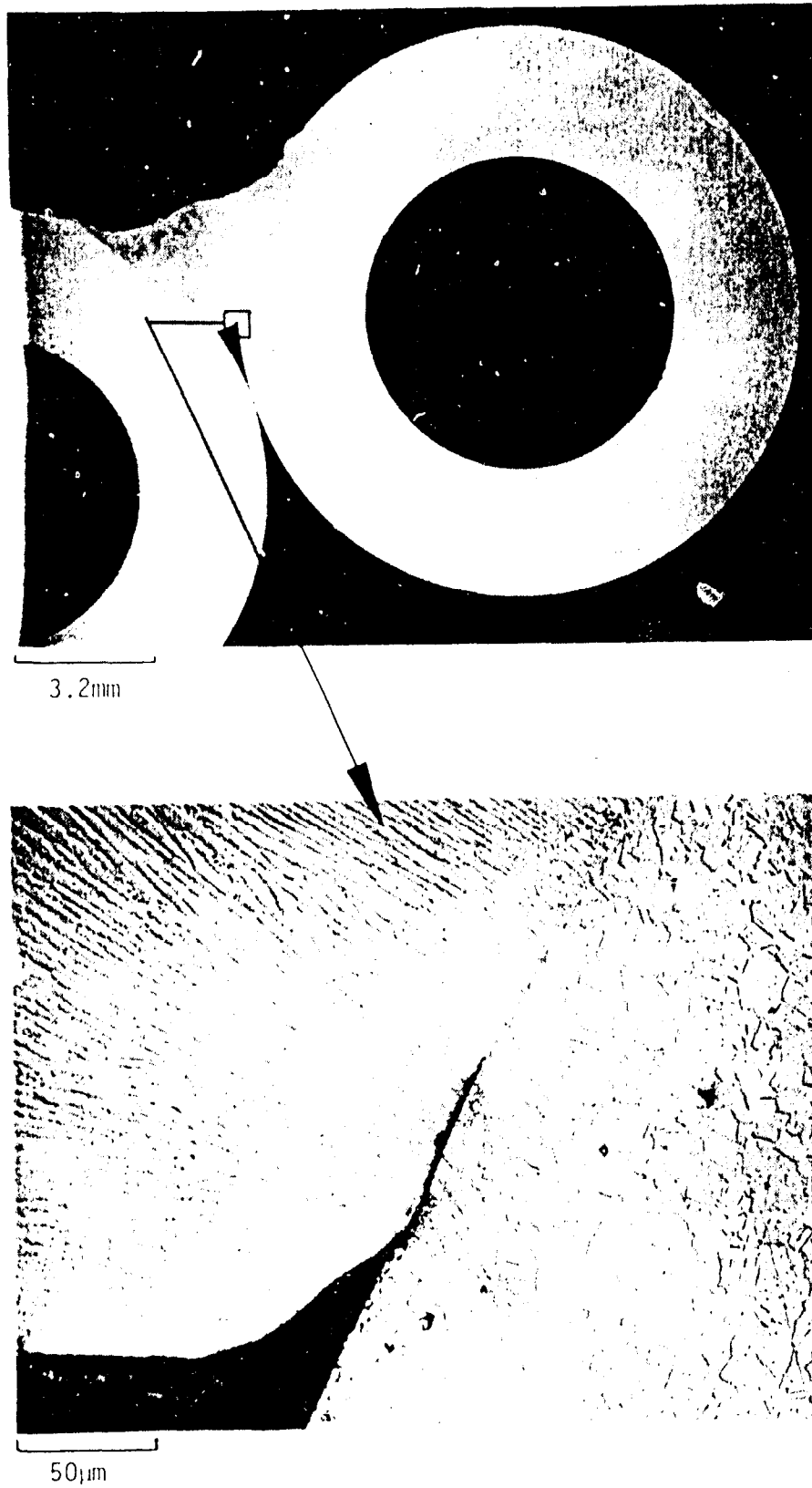


Figure 1. Micrograph of lack-of fusion weld defect prior to testing.

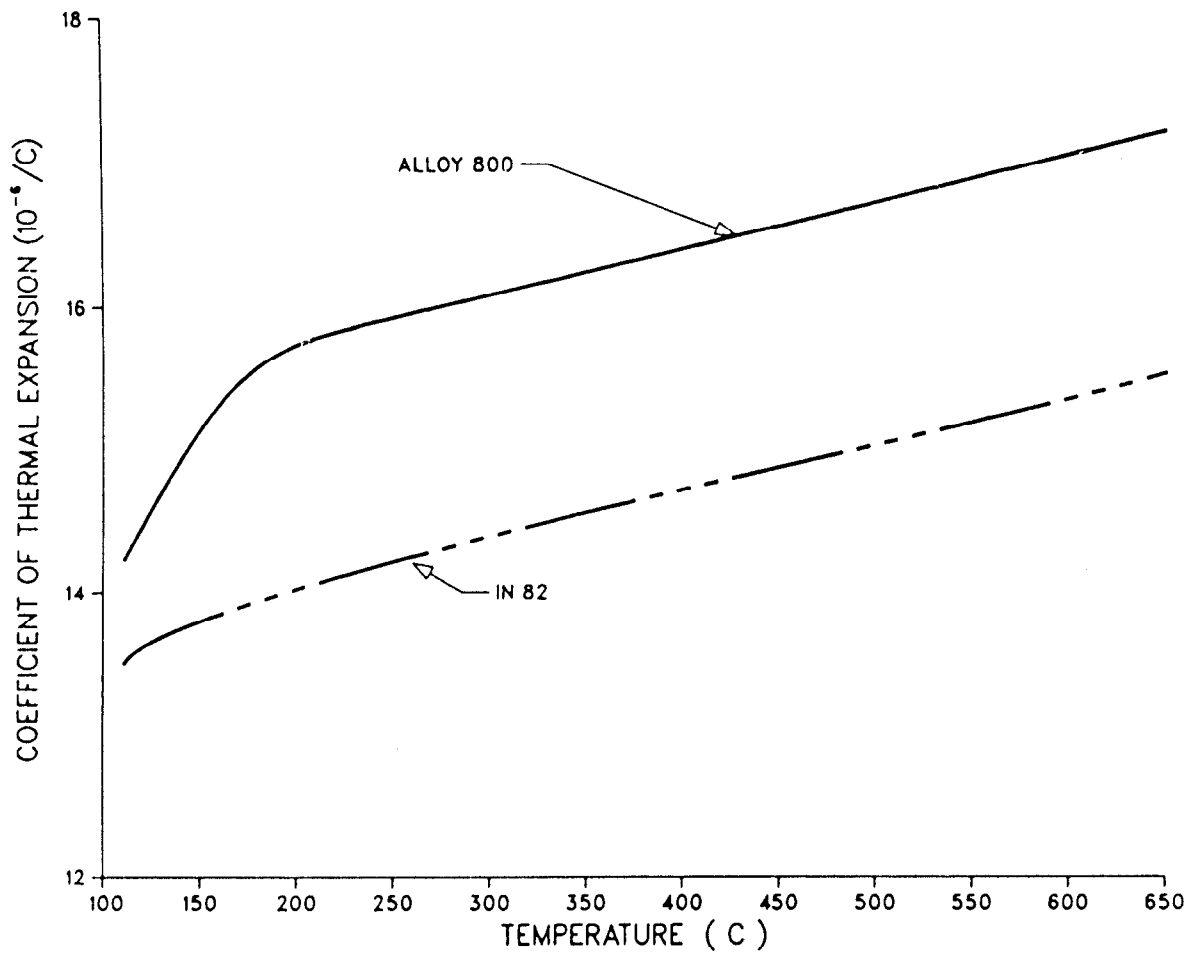


Figure 2. Average coefficient of thermal expansion for IN82 weld metal and alloy 800 versus temperature.

Experimental Procedures

All specimens were welded using the automatic gas-metal arc (GMA) process utilized for the pilot plant (see Appendix A for details). Prior to the GMA welds, gas-tungsten arc (GTA) tack welds were placed at the centers and ends of the specimens. The tack welds were used to provide a rigid structure for the subsequent automatic process and were also a part of pilot plant fabrication. A stepped fixture, in accordance with Rocketdyne's design, was used when welding to prevent bowing across the tube panels. After welding, the tube panels were straightened axially by cold bending. The presence of lack-of-fusion weld defects in the specimens was confirmed by metallographic examination of selected samples prior to testing (Fig. 1). Examination also revealed some solidification cracking in the GTA tack welds. Solidification cracks are easily identified by their intergranular nature.

In addition to evaluating the lack-of-fusion defects in continuous welds, the following specimen parameters were tested: the effect of welding stops and starts, end of weld-bead effects induced by the transition from plane strain to plane stress, bent-tube effects, and specimens with flaws intentionally introduced by electrical-discharge machining (EDM).

Thermal cycling during the experiment was induced by passing tube weldments alternately through a radiant lamp furnace and cooling chambers (Fig. 3 and 4). Weld panels 200 mm long, comprised of four tubes each, were attached in pairs at four stations as illustrated in Figure 5. The tube assemblies were mounted back-to-back with a support rack in between which admitted forced air inside the support rack to cool the back side of the weldments; this scheme created the necessary front-to-back ΔT on heating. The specimens were cycled on a timed basis, which included a three-minute stop in the furnace chamber to bring the specimens up to peak temperature; total cycle time was 15 minutes.

Temperatures during the test were measured on two end specimens. Thermocouples were placed on the specimens at four locations: 2 cm from each end on the furnace side and at the center on both the furnace and support side. A representative temperature history for one cycle of the tube crown on the front side of the panel and the weld bead on the back side of the panel is represented in Figure 6. During the test the front side of the panel, which is toward the radiant lamps, heats quickly and then is cooled quickly at the end of the cycle. On the other hand the back side (against the cooling rack) heats and cools more slowly during a cycle. This results in the required $\Delta T_{\text{front-back}}$ of 111°C at the peak temperature of the cycle. An initially large $\Delta T_{\text{front-back}}$ of 200°C and a negative $\Delta T_{\text{front-back}}$ of -100°C in the middle of the cycle also occur. The larger initial ΔT and the negative ΔT are more severe than the pilot plant conditions. However, they occur at lower temperatures where the yield strength is higher and thus probably do not contribute significantly to the accrued damage.

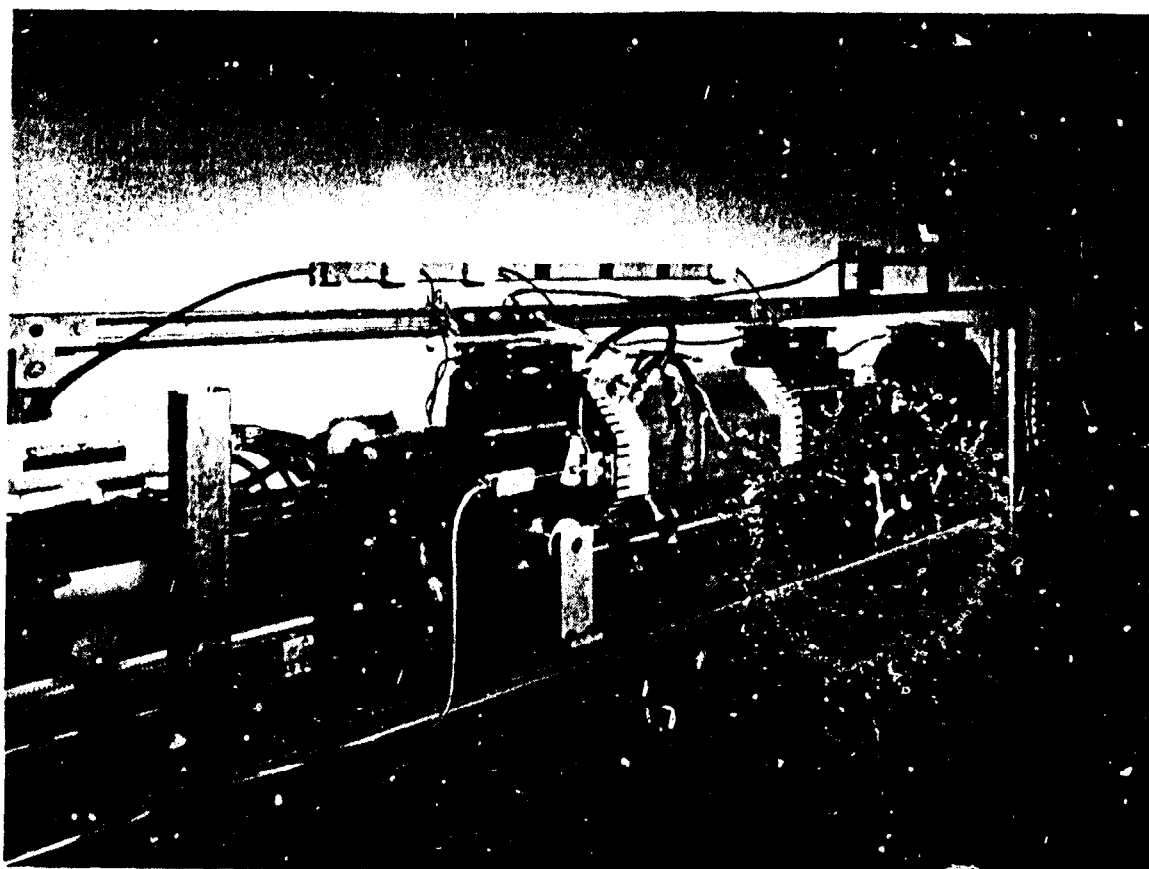
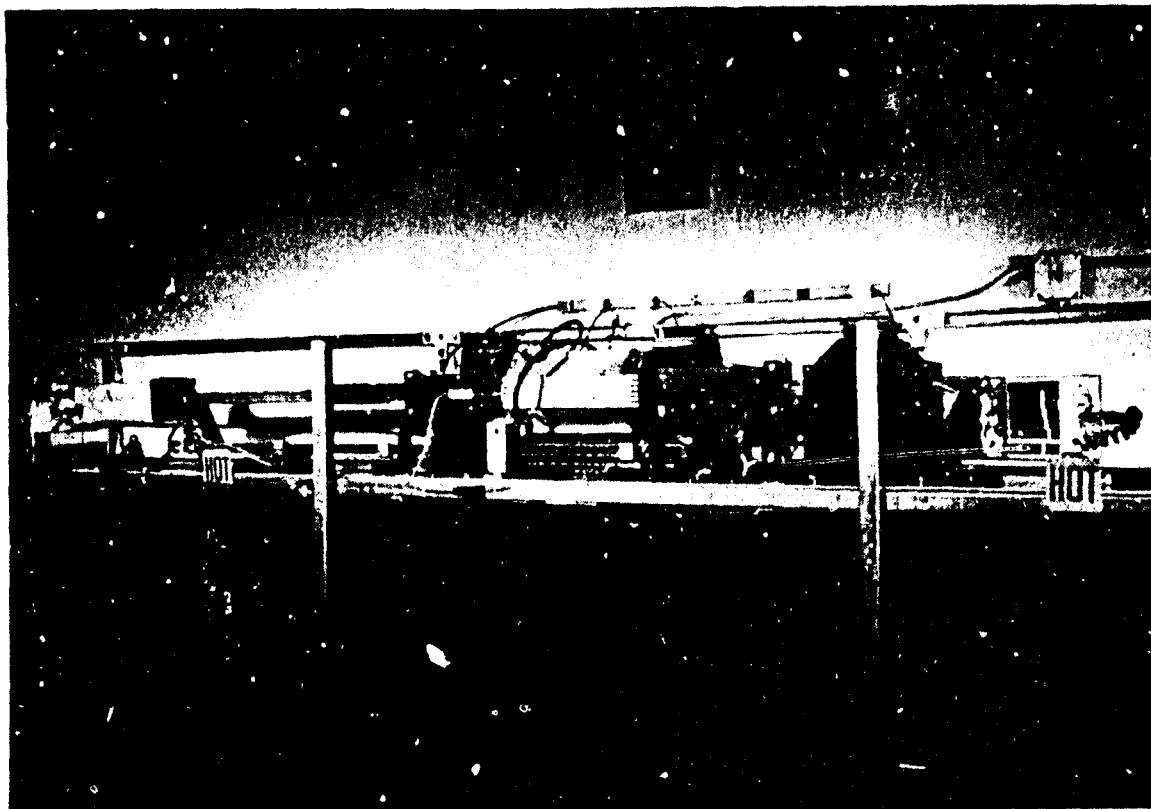


Figure 3. Thermal cycling apparatus for receiver tube weldments.

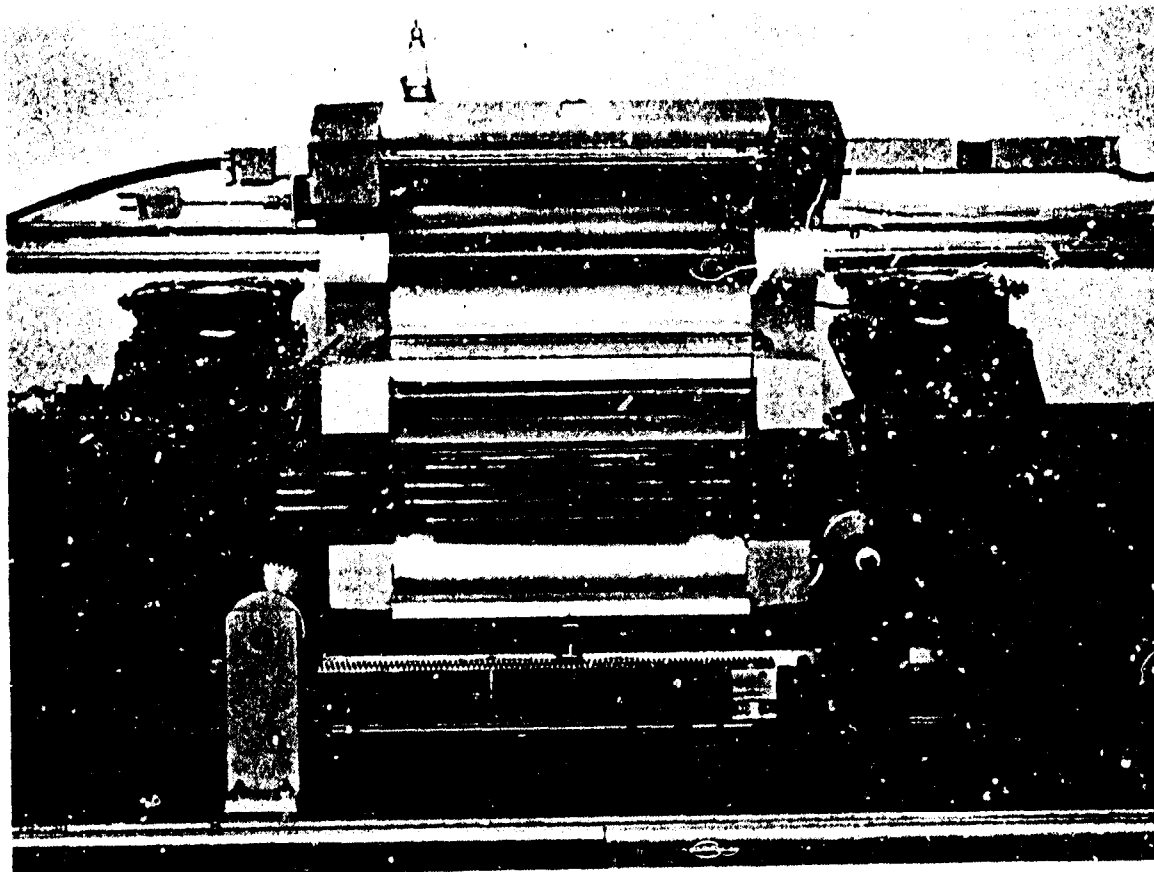


Figure 4. Close-up of radiant furnace and specimen.

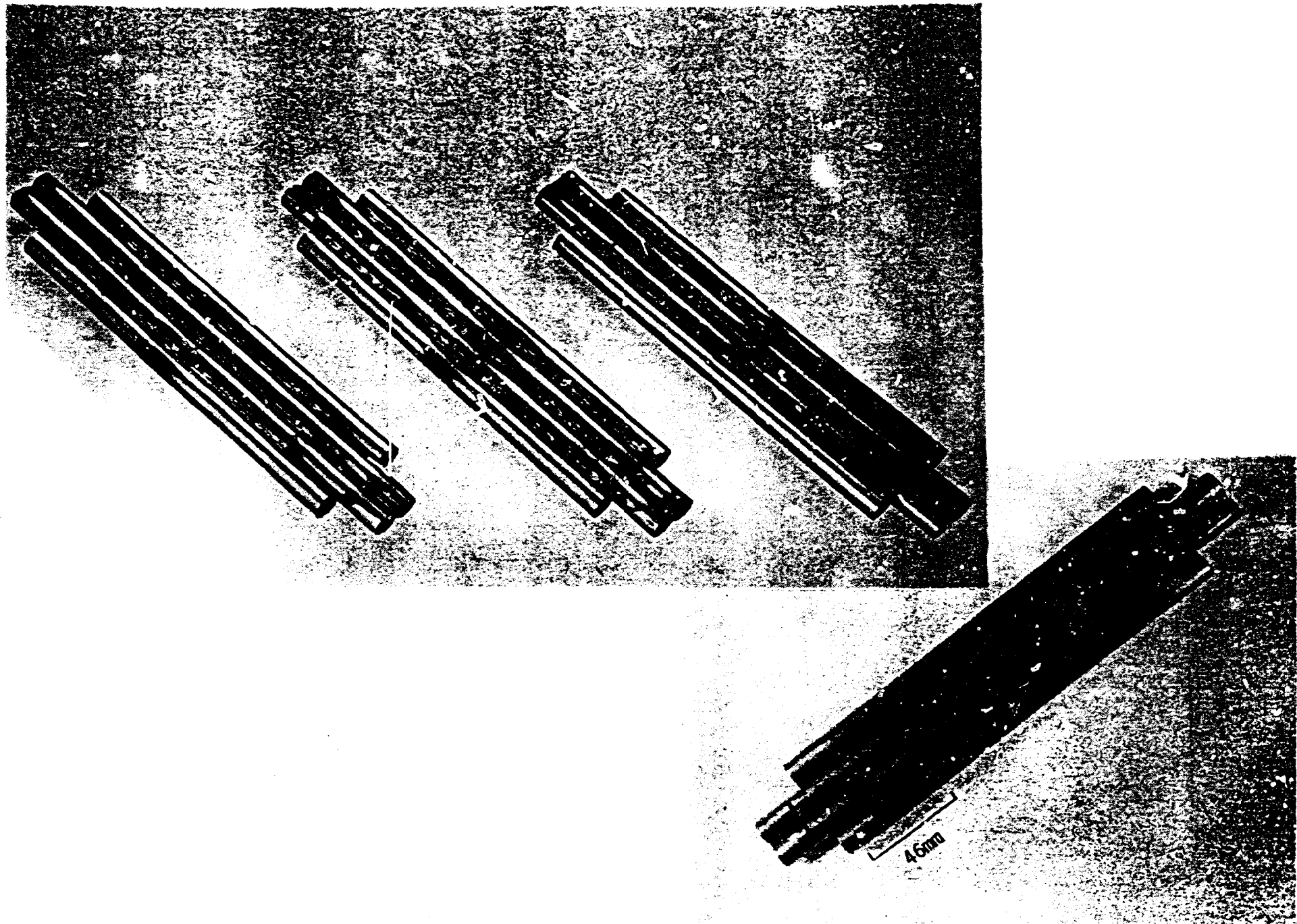


Figure 5. Receiver tube weldment specimens for test.

The minimum temperature in a cycle (Figure 6) was approximately 100°C. Peak temperature varied from cycle to cycle within an envelope of 12°C around 621°C due to fluctuations in ambient temperature (at the start of each set of 5000 cycles, this envelope was 40°C for the first few cycles before settling down to 12°C). The temperature distribution along the length of the specimens was also measured to determine the length of the temperature flat zone. At peak temperature this zone (Figure 7) was approximately 150 mm long for the first set of 5000 cycles, 100 mm for the second, and 200 mm for the third. The flat zone was not perfect for all of the tests because cold air entered through one side of the furnace (equivalent to right side of Figure 7). This flow of cold air from the cooling chambers was partially blocked in the first and third stages of the test. However, relocation of the apparatus in the laboratory prior to the second stage prevented us from blocking the flow of air during the second stage, thus the shorter temperature flat zone.

The test was conducted in three stages; during each stage, specimens were subjected to 5000 thermal strain cycles in the test apparatus. A total of 12 specimens was tested. Eight specimens were initially placed in the test apparatus. Of these first eight, two were removed after 5000 cycles, two after 10000, and four after 15000 for destructive examination. Four specimens were added to the test at the beginning of the second and third stages (two each time) to replace those removed for destructive examination. Thus, of the additional four, two had accumulated 5000 cycles and two had accumulated 10000 cycles by the end of the third stage. All specimens were then destructively examined to determine whether crack propagation had occurred.

Destructive examination was performed in two ways. The specimens were cross-sectioned randomly in several places and mounted for optical metallographic examination. Each mount was profiled through the cross section to maximize the possibility of discovering any cracks which might be present. A total of 100 profiles were made in twelve specimens. Also, small sections of the specimens were broken apart at the weld, thereby uncovering any crack propagation at the root of the weld. The fractured sections were first examined under a light microscope at 50X. Then any fractured surfaces which appeared to have large lack-of-fusion defects were examined with the SEM. Nondestructive inspection, such as x-ray and ultrasonic, was not possible because of specimen geometry.

Results and Discussion

Destructive examination of all samples did not reveal the occurrence of any crack propagation. It did confirm the expected presence of potential nucleation sites, i.e., lack-of-fusion defects and solidification cracks in the GTA tack welds. Figures 8 through 10 are micrographs of some typical lack-of-fusion defects from the tested specimens. These defects do not differ in any observable way from those in the untested condition, shown in Figure 1. An example of the solidification cracks is presented in Figure 11.

Typical Temperature History of Weldment Specimen for One Cycle

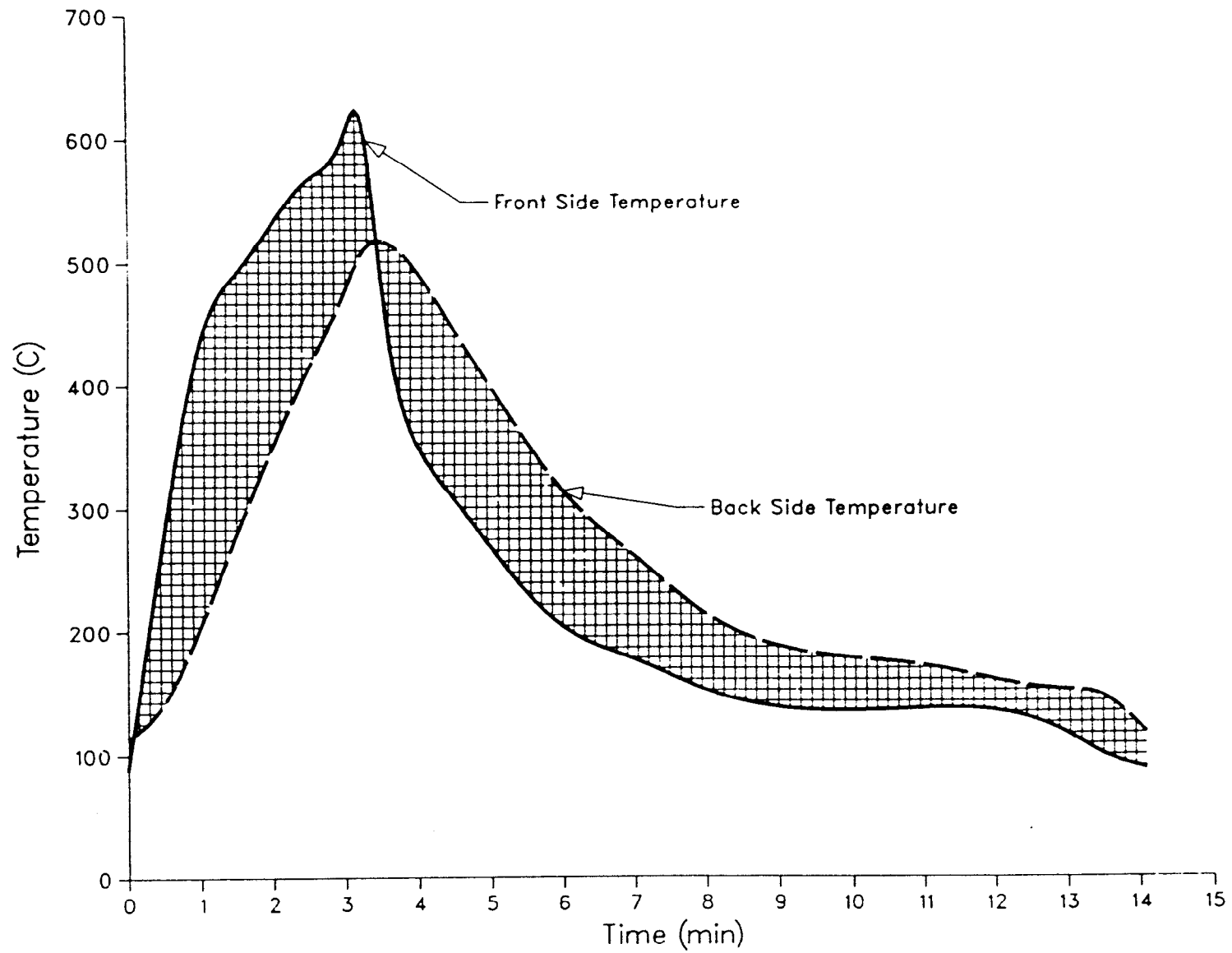


Figure 6. Typical temperature history of weldment specimen for one cycle.

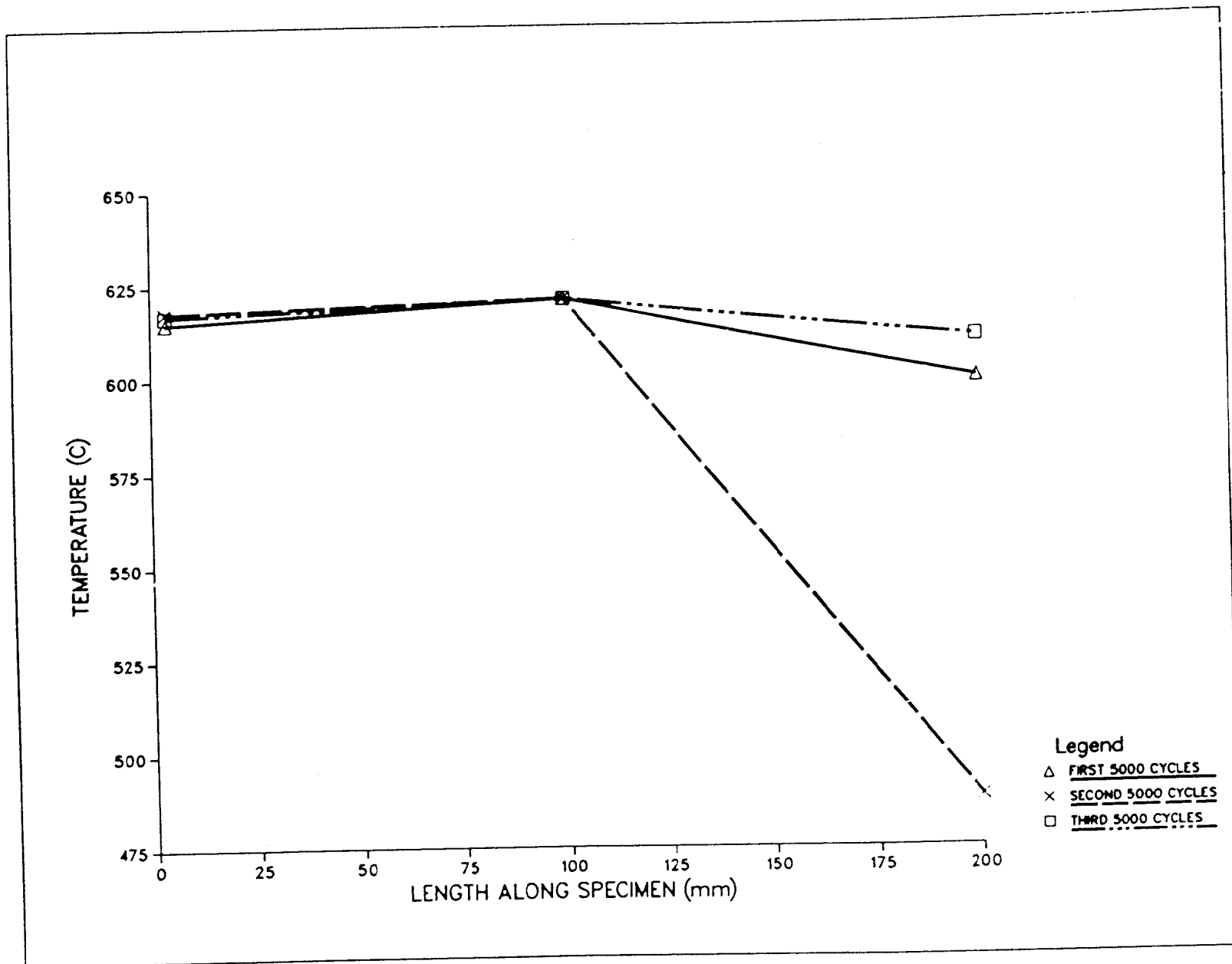
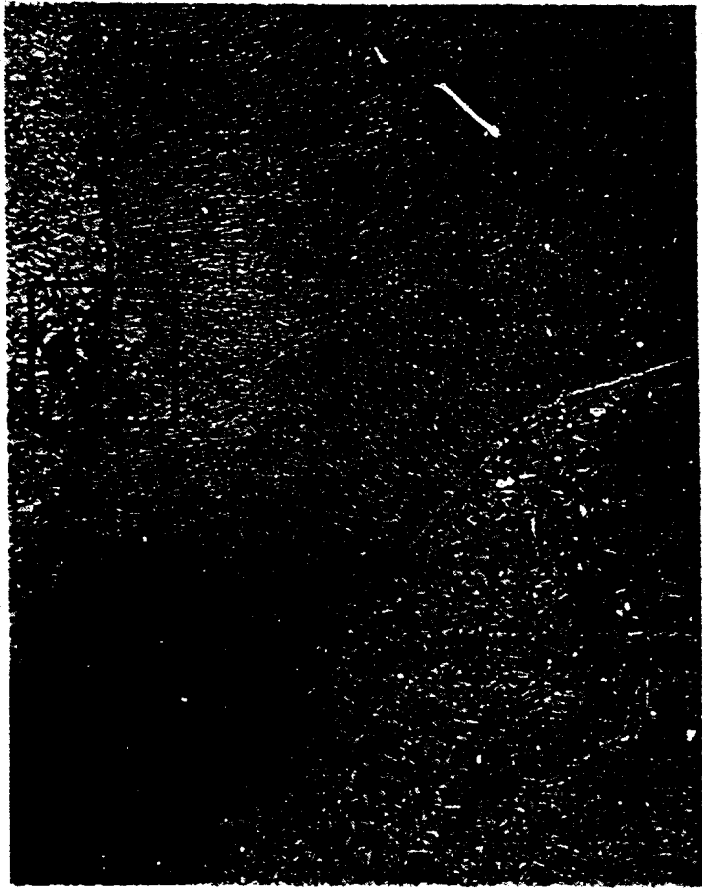
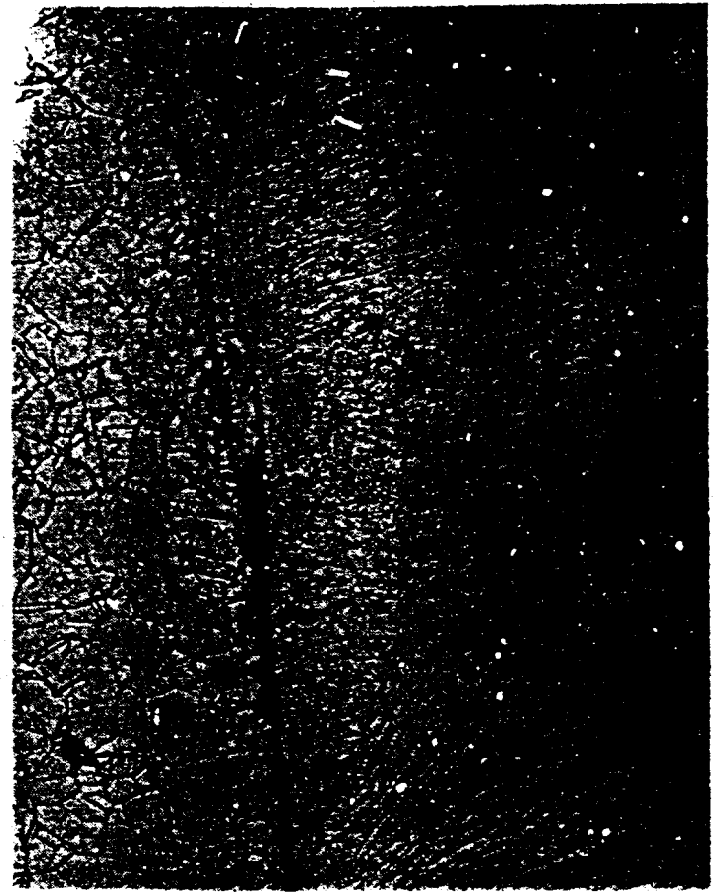


Figure 7. Variation of temperature along the length of specimens at peak temperature.



200 μm



50 μm

Figure 8. Lack-of-fusion weld defect, specimen removed after 10,000 cycles.

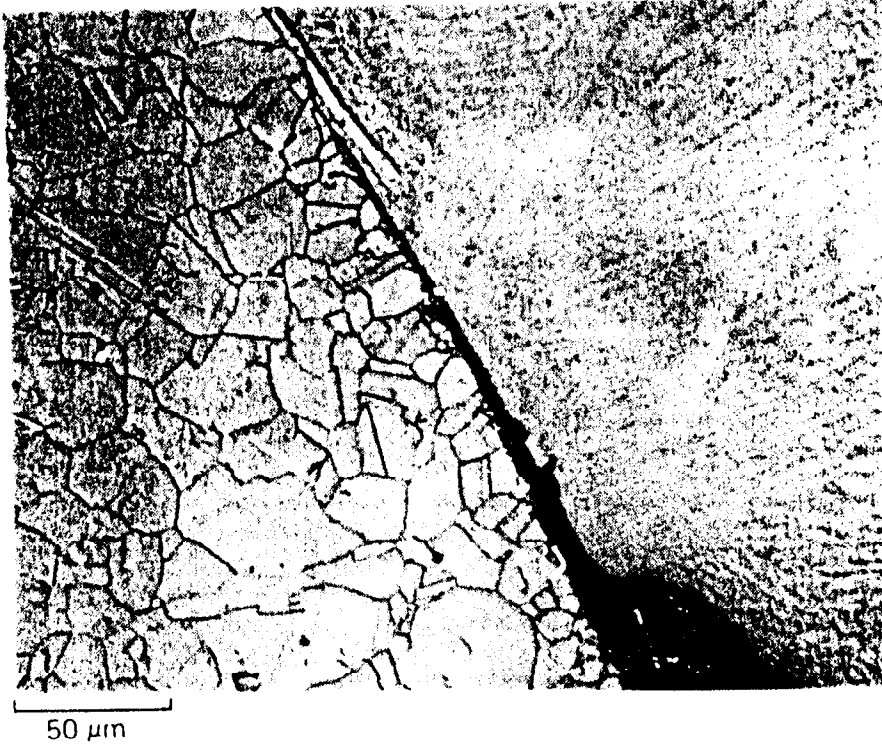
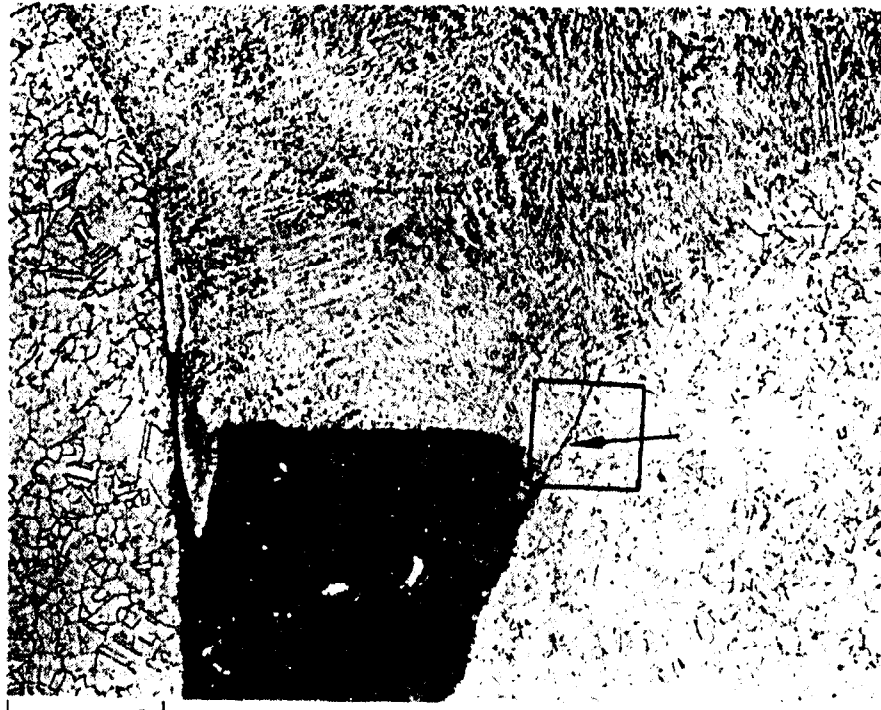
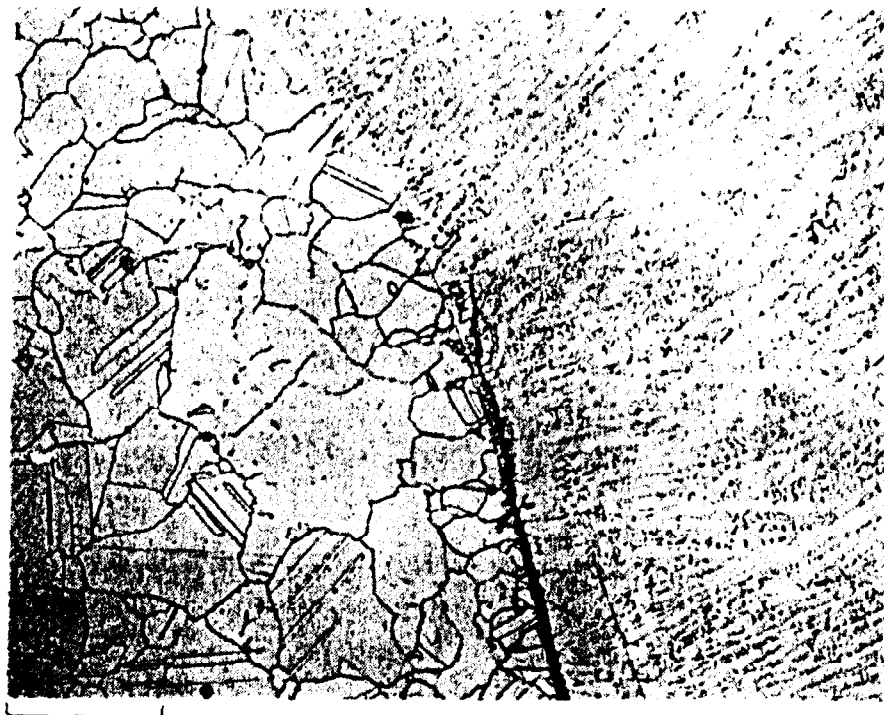


Figure 9. Lack-of-fusion weld defect, specimen removed after 10,000 cycles.

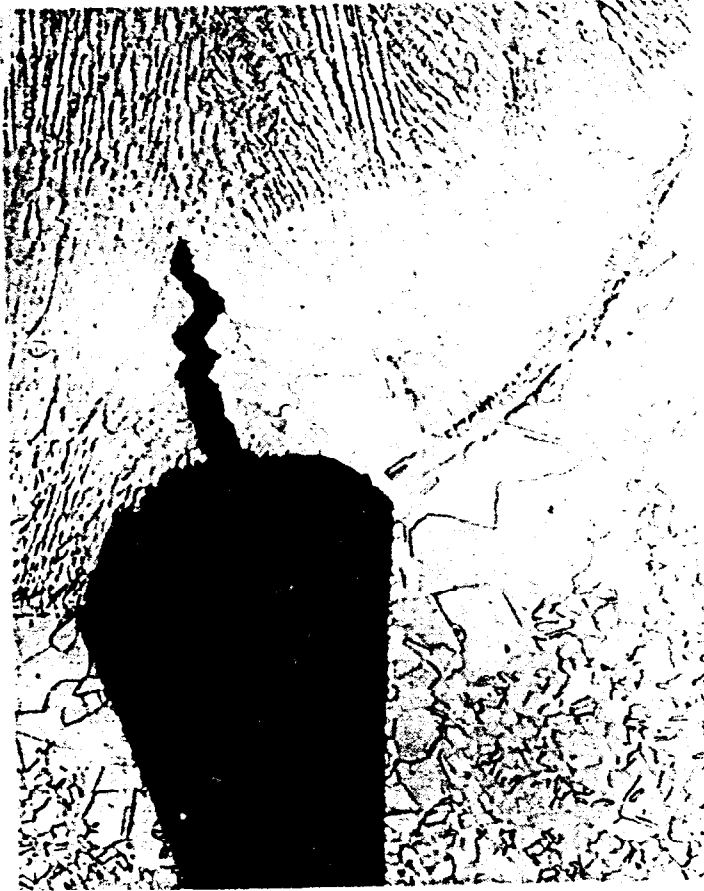


20µm



50µm

Figure 10. Lack-of-fusion weld defect, specimen removed after 15,000 cycles.



200 μm



50 μm

Figure 11. Example of solidification crack in GTA tack weld, crack occurred during welding. Specimen tested for 10,000 cycles.

EDM flaws were machined in two of the specimens; although these flaws increased local stresses by reducing the cross-sectional area of the interfaces, cracks still did not propagate as a result of these flaws (Figure 12). Although other weld parameters and tube configurations (as listed in previous section) were tested, no negative effects of these parameters could be identified since no cracks were found. Scanning electron microscopy of notched and fractured sections revealed a surface morphology reminiscent of that observed in the uncycled weldments, thus indicating that little or no crack propagation occurred during thermal cycling (Figure 13).

Discussion of the destructive examination results requires an evaluation of the imposed temperature distributions and thermal strain fields. As mentioned in the Introduction, the test operated at the maximum expected temperatures and $\Delta T_{\text{front-back}}$ for the "Solar One" central receiver. The resultant thermal strains, while dependent on the maximum temperature and on $\Delta T_{\text{front-back}}$, are also dependent on the amount of constraint against thermal expansion induced bending. The qualitative strain state and resultant stress state generated by this coupled effect is illustrated in Figure 14 for the region at the lack-of-fusion defect. This region is the site of large local stress concentrations because of the notch like characteristics of the defect. Thus, it is of most interest as the site of potential crack propagation.

The stress state at the lack-of-fusion defect/notch is a combination of Modes I (opening), II (shear), and III (anti-plane strain). Mode III, which contributes the largest component, has a nominal strain of approximately 0.1%. This strain component in the laboratory experiment is the same magnitude as for the receiver panel. It arises and was calculated from the difference in expansion coefficients between the weld and base metal. The smaller Mode I or crack opening strain component occurred in the test due to unconstrained bending of the tubes which open up the notch (Figure 14). Experiment design provided inadequate constraint against bending in the test for the first two sets of 5000 cycles. Increased constraint against bending was added for the third set of 5000 cycles. While the added constraint moves the experiment closer to actual receiver conditions and increases the nominal strains in the weldment, it actually decreases stress at the lack-of-fusion defects by removing the Mode I stress component.

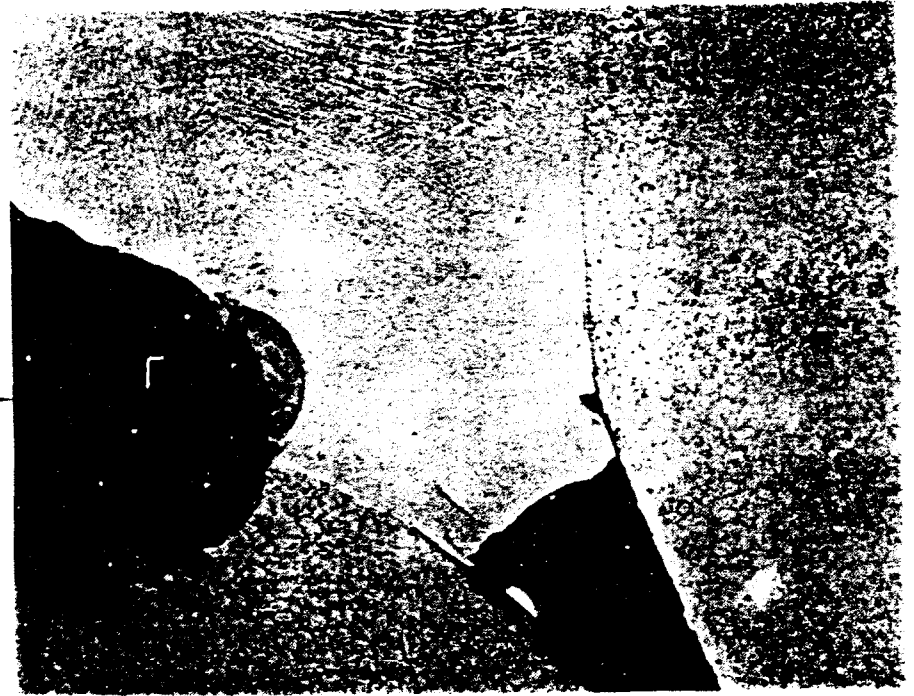
Weld residual stresses were initially present and similar to the receiver. These residual stresses were subsequently "annealed" out at the peak temperatures achieved during cycling. This annealing or stress relief should also occur in the receiver since the peak temperature of 650°C is in the temperature range for stress relief treatments for alloy 800.⁵

From consideration of the above discussion, the cyclic-strain state of the weldment specimens achieved in this test was reasonably representative of the cyclic strains in the receiver panel. Cracks did not propagate during the 15000 thermal strain cycles of this test.



200 μm

EDM
NOTCH



400 μm

Figure 12. EDM flaws and lack-of-fusion weld defect, specimen removed after 10,000 cycles.

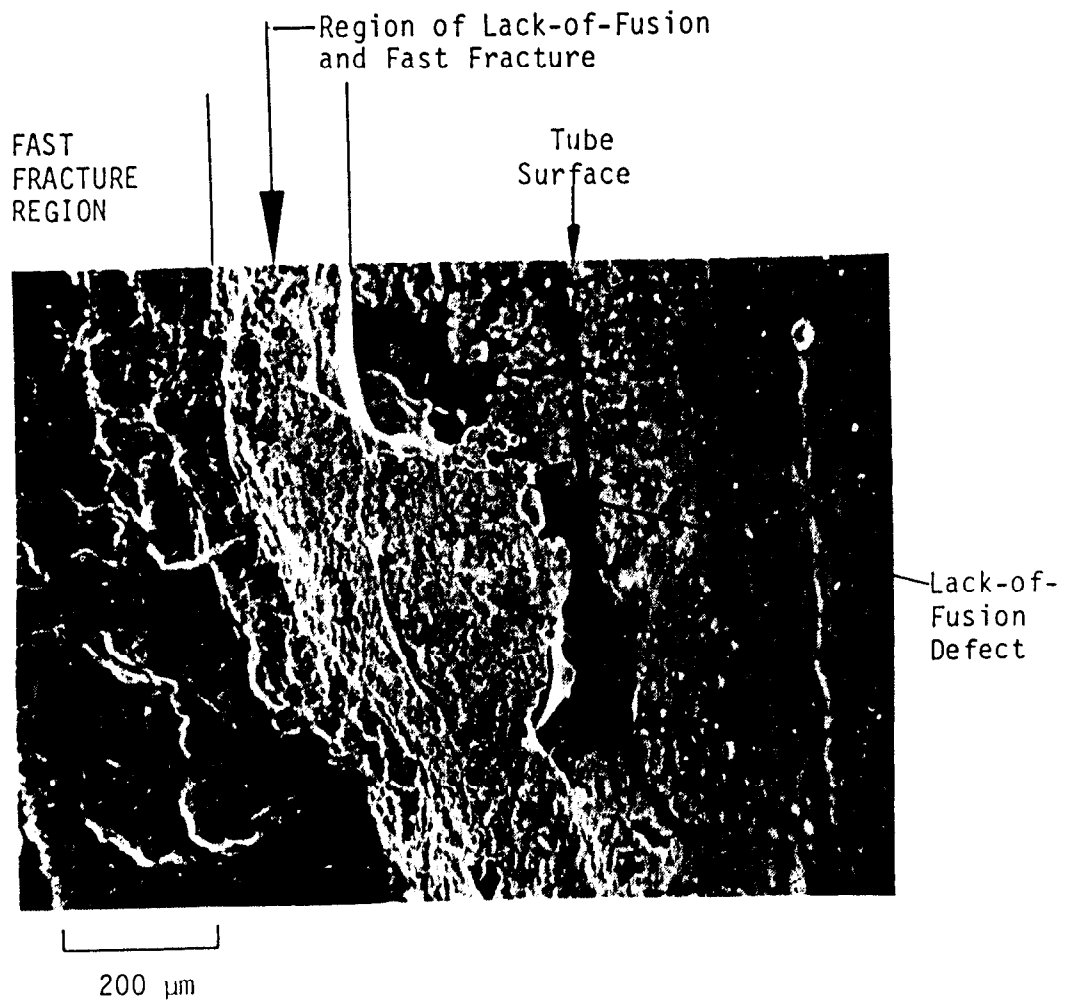


Figure 13. SEM micrograph of fractured surface showing lack-of-fusion region. Specimen notched and pulled apart after testing.

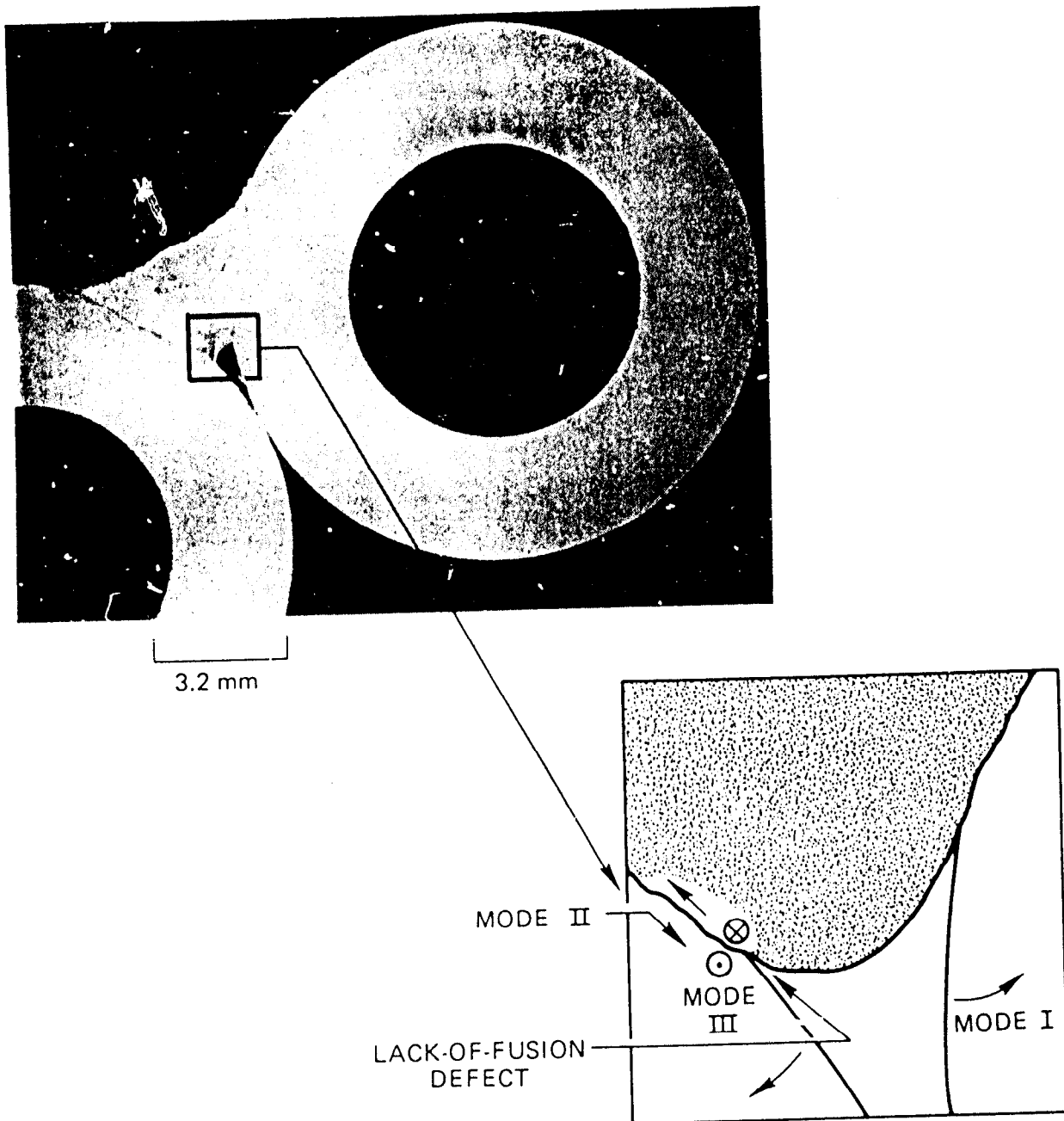


Figure 14. Schematic of strain/stress modes present at lack-of-fusion defects during test.

Summary and Conclusions

Receiver tube weldment specimens were subjected to a cyclic thermal strain environment similar to "Solar One" receiver conditions. The objective of this test was to determine whether crack propagation would occur at the lack-of-fusion weld defects as a result of this environment. Lack-of-fusion defects are present because of the low-heat input welding procedure chosen for fabrication of the receiver panels. If crack propagation occurred at these notch-like defects it could shorten the life of the receiver tube panels. However, metallographic examination of sectioned weldment specimens at the end of the 15,000 cycles did not reveal that any crack propagation had occurred.

REFERENCES

1. J. Jones, Effects of Bending on the Fatigue Life of Solar Receiver Tubes Subjected to One-Sided Heating, SAND78-8038, February 1979.
2. MDAC/Rocketdyne Solar Receiver Design Review, SAND78-8188, November 1978.
3. Performance Analysis for the MDAC Rocketdyne Pilot and Commercial Plant Solar Receivers, SAND78-8183, September 1978.
4. Private communication, R. Fish, Rocketdyne, 1980.
5. Huntington Alloys Technical Bulletins, Incoloy Nickel-Iron-Chromium Alloys and Inconel Nickel Alloys, 20M 6-78 T-40 and 10M 8-77 S-9.

APPENDIX A

MATERIAL: Incoloy 800

FILLER WIRE: Inconel 82: (0.89mm diameter)

EQUIPMENT: Linde SVI-600 CV/DC Power Supply, ST-21 torch, Side Beam

WELD REQUIREMENTS: ASME Sec. IX

CURRENT: 140 AMPS

TRAVEL SPEED: 38 IPM

VOLTAGE: 22 V

WIRE FEED: 350 IPM

SHIELDING GAS: 75% HE - 25% AR

FLOW RATE: 50 CFH

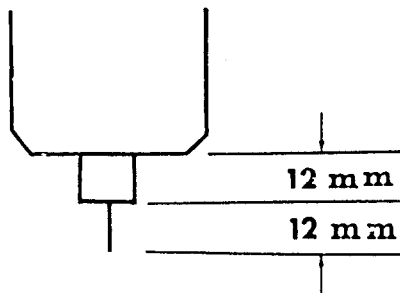
INDUCTANCE: 4.75 (on Linde SVI-600)

SLOPE: 3 (on Linde SVI-600)

WIRE SIZE: .89 mm

CUP SIZE: 25 mm I.D.

STICKOUT LENGTH:



JOINT DESIGN:

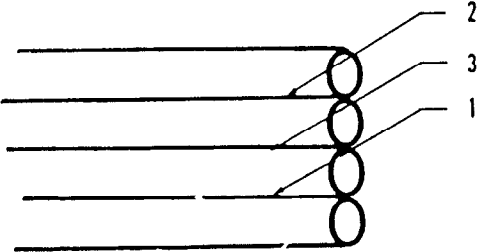


DEVELOPMENT PROCEDURE:

1. Clean tubes with Acetone.
2. Tack tubes with 9 mm long welds as concave as possible.
3. Reclean surface with Acetone.
4. Punch mark starts and stops of tack welds on outside of tubes.
5. Start with weld sequence.

APPENDIX A (continued)

WELD SEQUENCE: (For straight tubes)



UNLIMITED RELEASE

INITIAL DISTRIBUTION

U. S. Department of Energy
Division of Solar Thermal Technology
James Forrestal Building
1000 Independence Avenue. S.W.
Washington, D. C. 20585
Attn: W. W. Auer
G. W. Braun
K. T. Cherian
C. B. McFarland
J. E. Rannels

U. S. Department of Energy
San Francisco Operations Office
Division of Solar Technology
1333 Broadway
Oakland, CA 94612
Attn: S. D. Elliott
R. W. Hughey

U. S. Department of Energy
San Francisco Operations Office
Solar Ten Megawatt Project Office
5301 Bolsa Avenue MS 14-1
Huntington Beach, CA 92647
Attn: R. N. Schweinberg

Aerospace Corporation
P.O. Box 92957
Los Angeles, CA 90009
Attn: P. Mathur

Babcock & Wilcox
20 S. Van Buren Avenue
Barberton, OH 44203
Attn: O. W. Durrant
G. Grant

Bechtel Corporation
P.O. Box 3965
San Francisco, CA
Attn: E. Lam

Black & Veatch Consulting Engineers
P.O. Box 8405
Kansas City, MO 64114
Attn: J. E. Harder
J. C. Grosskreutz

Combustion Engineering, Inc.
1000 Prospect Hill Road
Windsor, Connecticut 06095
Attn: H. M. Payne

Foster Wheeler Development Corporation
12 Peach Tree Hill Road
Livingston, NJ 07039
Attn: R. J. Zoschak
T. V. Narayanan
A. C. Gangadharan
I. Berman

General Electric Co.
Energy Systems and Technology Division
310 DeGuigne Drive
Sunnyvale, CA 94086
Attn: Sig Wolf

Martin Marietta Corporation
P.O. Box 179
Denver, CO 80201
Attn: T. R. Tracey

McDonnell Douglas
5301 Bolsa Avenue
Huntington Beach, CA 92647
Attn: G. Coleman
R. Gervais
R. Easton
R. Hallet

Rockwell International
Energy Systems Group
P.O. Box 1449
8900 DeSoto Avenue
Canoga Park, CA 91304
Attn: T. S. Springer

Rockwell International
Rocketdyne Division
6633 Canoga Avenue
Canoga Park, CA 91304
Attn: J. M. Friefeld

Southern California Edison
P.O. Box 800
Rosemead, CA 91770
Attn: J. Reeves
C. Winarski
P. Skvarna
K. Ross

Stearns-Roger
P.O. Box 5888
Denver, CO 80217
Attn: W. R. Lang

J. H. Scott, 4700
D. G. Schueler, 4720
J. V. Otts, 4722
T. B. Cook, 8000; Attn: D. M. Olson, 8100
A. N. Blackwell, 8200

C. S. Hoyle, 8122
L. Napolitano, 8122
M. Abrams, 8124
R. J. Gallagher, 8124
B. F. Murphey, 8300; Attn: R. L. Rinne, 8320
G. W. Anderson, Jr., 8330
W. Bauer, 8340

D. M. Schuster, 8310
D. A. Nissen, 8312
P. J. Royval, 8312
R. W. Mar, 8313
A. J. West, 8314
S. L. Robinson, 8314
D. V. Zanini, 8314
L. A. West, 8315
J. C. Swearngen, 8316
D. A. Hughes, 8316 (10)
L. Gutierrez, 8400
R. C. Wayne, 8430
C. T. Yokomizo, 8451
A. C. Skinrood, 8452
J. J. Bartel, 8452
E. T. Cull, 8452
W. G. Wilson, 8453

Publications Division, 8265, for TIC (27)
Publications Division, 8265/Technical Library Processes and Systems Division, 3141
Technical Library Processes Division, 3141 (3)
M. A. Pound, 8214, for Central Technical Files (3)